Eur. Phys. J. A (2024) 60:220
https://doi.org/10.1140/epja/s10050-024-01436-x

THE EUROPEAN PHYSICAL JOURNAL A

Regular Article - Experimental Physics

Neutron transfer in ^{7}Li+^{205}Tl system

Prasanna M.[1], V. V. Parkar[2,3,a], V. Jha[2,3], S. K. Pandit[2,3], A. Parmar[4], A. Shrivastava[2,3], K. Mahata[2,3], K. Ramachandran[2], R. Palit[5], Bhushan Kanagalekar[1], B. G. Hegde[1,b]

[1] Department of Physics, Rani Channamma University, Belagavi 591156, India
[2] Nuclear Physics Division, Bhabha Atomic Research Centre, Mumbai 400085, India
[3] Homi Bhabha National Institute, Anushaktinagar, Mumbai 400094, India
[4] Department of Physics, Faculty of Science, The M. S. University of Baroda, Vadodara 390002, India
[5] Department of Nuclear and Atomic Physics, Tata Institute of Fundamental Research, Mumbai 400005, India

Received: 23 September 2024 / Accepted: 8 October 2024

Communicated by Alessia Di Pietro

Abstract Neutron transfer cross sections for ^{7}Li+^{205}Tl system were measured near Coulomb barrier energies using online γ-ray detection technique. One neutron stripping, two neutron stripping, and one neutron pickup cross sections have been extracted and are compared with the Coupled Reaction Channel (CRC) calculations. The systematics of one and two neutron stripping and pickup cross sections with a ^{7}Li projectile on several targets show an approximate universal behaviour. A comparison of integrated neutron transfer cross sections with complete and incomplete fusion cross sections available with ^{7}Li projectile is presented to understand the systematic behaviour. The neutron transfer along with cumulative sum of complete and incomplete fusion was found to explain the estimated reaction cross section in ^{7}Li+^{205}Tl system.

1 Introduction

Over the past few decades, the study of heavy-ion induced reactions with stable weakly bound nuclei has gained importance for understanding the fundamental nuclear features related to structure and reaction dynamics [1–7]. These studies help in exploring reactions involving more exotic nuclei and radioactive ion beams. In this regard, reaction phenomenon particularly fusion, elastic scattering, inelastic excitation, breakup reactions etc., have been studied extensively for these nuclei. Additionally, measurement of direct nuclear transfer reactions involving the stable weakly bound nuclei (^{6,7}Li, ^{9}Be) have been performed and the significance of nucleon transfer in the reaction dynamics has been investigated in several studies [8–20]. In the subsequent studies, based on neutron transfer cross sections available with ^{6,7}Li and ^{9}Be projectiles on various targets [15,21,22], it was concluded that there is no dependence on target structure. The projectile structure plays a major role in the transfer process; viz; the highest neutron stripping cross section is obtained with ^{9}Be (S_n = 1.67 MeV) projectile followed by ^{6}Li (S_n = 5.67 MeV) and ^{7}Li (S_n = 7.25 MeV) projectile nuclei.

The transfer of a single valence nucleon or a group of nucleons collectively at the periphery of the colliding partners are known to affect the fusion cross sections at energies near the Coulomb barrier due to presence of significant coupling effects of single particle and continuum of states. The enhancement in fusion cross sections at near barrier energies could also be explained considering the neutron flow model of Stelson [23,24]. This model is based on the neutron flow due to the exchange of neutrons between the interacting projectile and target nuclei and its usefulness has been demonstrated in various studies of fusion reactions with many projectiles [25–29].

Often, nucleon transfer is followed by various breakup modes of the projectile [30], with fragments potentially being absorbed by the target. There is a large probability that some of the breakup fragments may be subsequently absorbed in the field of the target leading to the process called as breakup fusion which makes contributions towards incomplete fusion (ICF). Some of other contributions to ICF can be ascribed to the transfer of the nucleons to the high-lying states in the continuum of the target. Separating the effects of transfer and breakup processes can be challenging, making it essential to understand them in a unified way. Further, knowledge about relative importance of the breakup and transfer processes and their contribution to the ICF, CF and reaction cross section is

[a] e-mail: vparkar@barc.gov.in (corresponding author)
[b] e-mail: bghegde@rcub.ac.in

Published online: 09 November 2024

important for obtaining a better understanding of the reaction mechanism.

In recent times, various new theoretical models have been developed and employed for describing the data and obtaining the understanding of breakup-transfer processes for weakly bound nuclei. For the breakup reactions, the Continuum Discretized Coupled Channels (CDCC) has proved to be one of the most successful approaches for describing coupling effects due to breakup of nucleon(s) of the projectile nucleus. While the elastic part of the breakup is described very successfully through the CDCC method, the non-elastic breakup is not so easy to calculate. In recent times, the IAV and its extensions have been developed for modelling the inelastic breakup [31–34]. Extensions to CDCC have been also been made for calculating the ICF [12,13,35–40], where one of the fragments of the projectile is considered to be transferred to the target. Coupled Reaction Channel (CRC) calculations have been employed for studying the effect due to transfer channels and significant coupling effects due to one neutron transfer has been found in many systems [15–18,21,22].

With this motivation, neutron transfer in ^{7}Li+^{205}Tl system near Coulomb barrier energies have been studied, utilizing online γ-ray measurement and the results are compared with Coupled Channel (CC) calculations. Further, systematics of ^{7}Li induced reactions on several target systems along with the present data is studied. The paper is organised as follows. The experimental details are given in Sect. 2. The experimental results and the calculation details are given in Sect. 3 followed by the summary in Sect. 4.

2 Experimental details

The details of the experimental setup are given in our earlier work [41] and only a short summary is given here for completeness. The experiment was performed using ^{7}Li beam from the BARC-TIFR Pelletron LINAC Facility, Mumbai, India at ten energy points in the energy range E_{beam} = 25-40 MeV. The target ^{205}Tl of 1 mg/cm^2, evaporated on 25 μg/cm^2 carbon backing was placed inside a compact chamber made of aluminium alloy, surrounded by Indian National Gamma Array (INGA) setup [42]. The array was consisting of nine Compton suppressed High Purity Germanium (HPGe) Clover detectors for detection of γ-rays from the residues populated in ^{7}Li+^{205}Tl reaction. Inside the chamber, three charged particle detector telescopes (ΔE = 25 − 40 μm, E = 1000 μm) were placed at 70°, 120° and 140°, respectively for detection of elastic and α particle events mainly. In addition, two Si surface barrier detectors with thicknesses 300 μm, acting as monitor detectors were also placed at ± 25° for absolute normalisation purpose. The time stamped data were collected using a digital data acquisition system with a sampling rate of 100 MHz [42]. Standard calibrated radioactive ^{152}Eu and ^{133}Ba sources were used for efficiency and energy calibration of the clover detectors. Figure 1 shows the typical γ-ray add-back spectrum from all the clover detectors measured at E_{beam} = 38 MeV for ^{7}Li+^{205}Tl system. The prompt γ-rays from one neutron stripping (^{206}Tl), two neutron stripping (^{207}Tl) and one neutron pickup (^{204}Tl) channel are labeled.

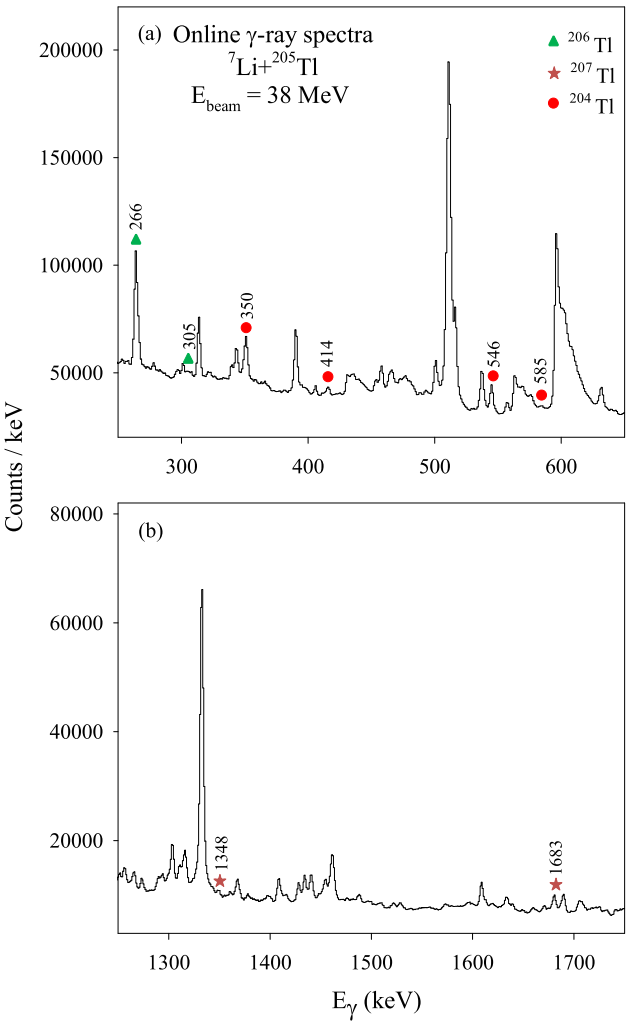

Fig. 1 γ-ray add-back spectrum from all the clover detectors obtained in ^{7}Li+^{205}Tl system at E_{beam} = 38 MeV. The γ lines following one neutron stripping (^{206}Tl), two neutron stripping (^{207}Tl) and one neutron pickup (^{204}Tl) channels are marked

3 Results and discussion

3.1 Data Reduction

The data reduction procedure for extraction of residue cross sections is similar as given in our previous work [41]. The cross sections for residues from one neutron stripping ^{206}Tl,

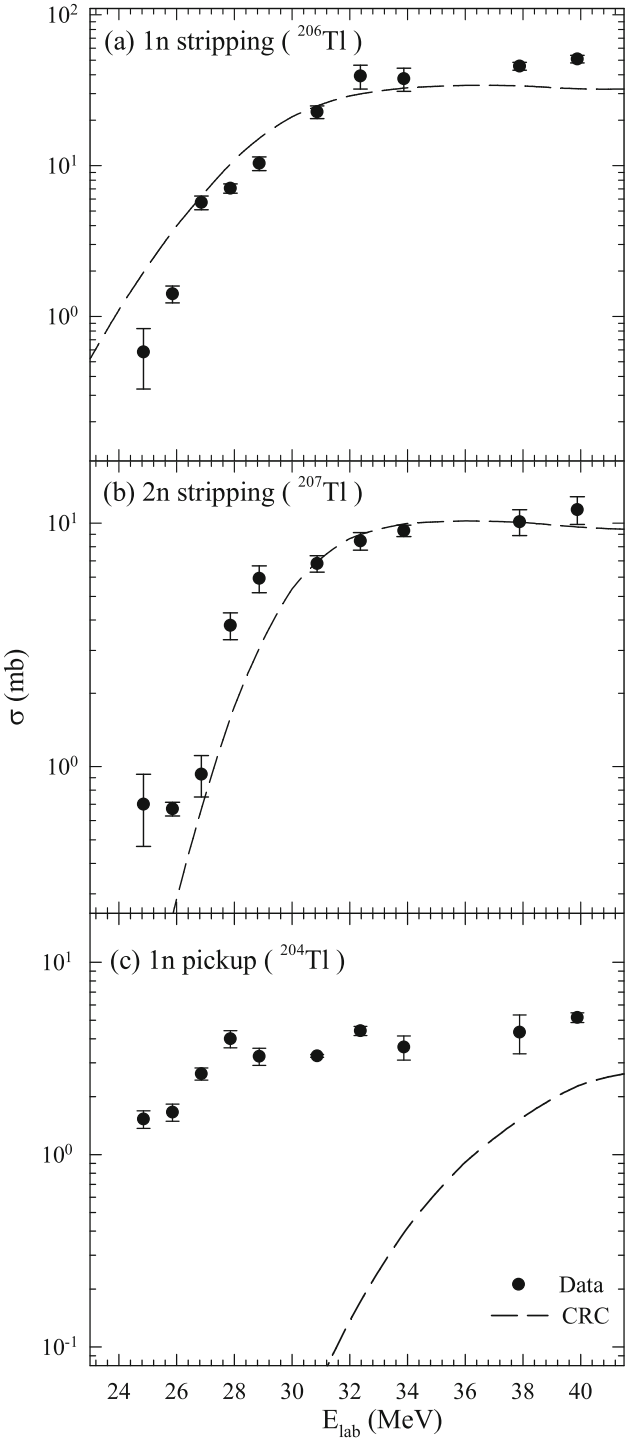

Fig. 2 Measured (**a**) one neutron stripping, (**b**) two neutron stripping and (**c**) one neutron pickup transfer cross sections in the ^{7}Li+^{205}Tl system are compared with CRC calculations

Table 1 Measured one neutron stripping, two neutron stripping and one neutron pickup cross sections in ^{7}Li+^{205}Tl system

E_{lab} (MeV)	^{206}Tl (mb)	^{207}Tl (mb)	^{204}Tl (mb)
24.9	0.58 ± 0.25	0.70 ± 0.23	1.53 ± 0.16
25.9	1.41 ± 0.18	0.67 ± 0.04	1.66 ± 0.17
26.9	5.69 ± 0.59	0.93 ± 0.18	2.63 ± 0.19
27.9	7.06 ± 0.50	3.80 ± 0.48	4.00 ± 0.40
28.9	10.35 ± 1.08	5.93 ± 0.75	3.24 ± 0.33
30.9	22.70 ± 2.2	6.82 ± 0.53	3.26 ± 0.06
32.4	39.27 ± 7.09	8.44 ± 0.70	4.40 ± 0.24
33.9	37.69 ± 6.58	9.31 ± 0.50	3.62 ± 0.52
37.9	45.66 ± 2.74	10.12 ± 1.23	4.33 ± 1.00
39.9	50.92 ± 2.98	11.35 ± 1.48	5.16 ± 0.30

two neutron stripping ^{207}Tl and one neutron pickup ^{204}Tl, were determined considering the prompt γ-ray transitions populating the ground and metastable states. The information of γ lines populating the ground and metastable states in these nuclei is taken from Refs. [43,44]. The cross sections for one neutron stripping ^{206}Tl, two neutron stripping ^{207}Tl and one neutron pickup ^{204}Tl are shown in Fig. 2(a–c) and are also listed in Table 1. As can be seen, one neutron stripping cross sections are higher than other transfer channels.

The measured elastic scattering cross sections normalized to the Rutherford cross sections were obtained by taking the ratio of yields of elastic to the yield of the monitor detector. The measured elastic scattering angular distribution at three angles for ^{7}Li+^{205}Tl system at different bombarding energies are shown in Fig. 3. These angular distributions were utilized for testing entrance channel potentials used in the Coupled Channel calculations (discussed later) and also to get the reaction cross sections.

3.2 Coupled channel calculations

Coupled channel calculations, namely Coupled Reaction Channel (CRC) and Continuum Discretized Coupled Channel (CDCC) were performed to understand the mechanism of neutron transfer and breakup reactions respectively. Detailed discussion of these kind of calculations was given in our earlier works [21,22]. Measured elastic scattering data was utilized for testing our entrance channel potentials and also

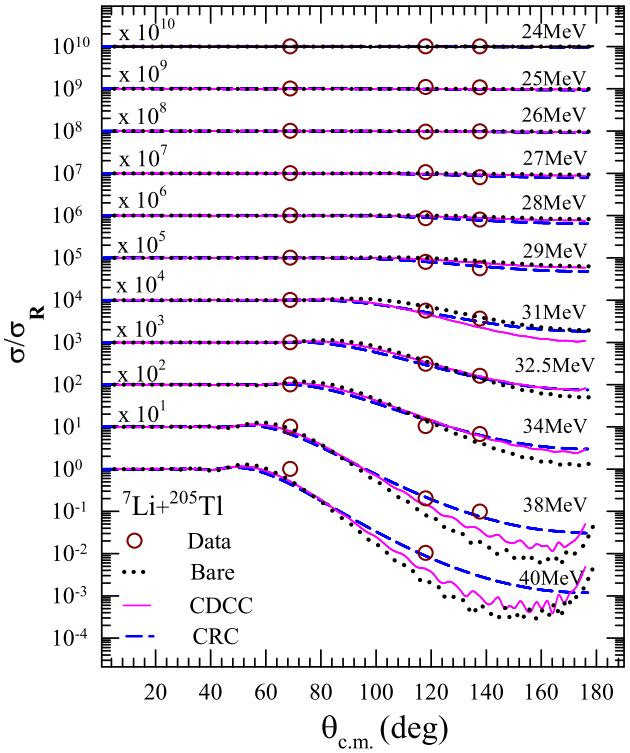

Fig. 3 Measured elastic scattering angular distribution data for the ^{7}Li+^{205}Tl system are compared with the calculations (see text for details)

to see the effect of breakup couplings on the elastic scattering angular distributions. These calculations were performed using FRESCO code (version FRES 2.9) [45].

3.2.1 CRC calculations

CRC calculations for one neutron stripping, two neutron stripping and one neutron pickup were performed by using the global phenomenological optical model potentials of which the parameters are given in Table 2. The potentials binding the transferred particles were of Woods-Saxon volume form, with radius $1.25A^{1/3}$ fm and diffuseness 0.65 fm, with 'A' being the mass of the core nucleus. The depths were adjusted to obtain the required binding energies of the particle-core composite system. The single particle states along with spectroscopic factors (C^2S) taken from [46–50] considered in the calculations are given in Table 3. For the ^{7}Li $\rightarrow$ ^{6}Li transfer, both the $1p_{3/2}$ and $1p_{1/2}$ components of the neutron bound to ^{6}Li were included with spectroscopic factors of C^2S = 0.43 and 0.29 respectively, taken from Cohen and Kurath [51]. Similarly for ^{7}Li $\rightarrow$ ^{8}Li transfer, both the $1p_{3/2}$ and $1p_{1/2}$ components of the neutron bound to ^{7}Li were included with spectroscopic factors of C^2S = 0.98 and 0.056 respectively, taken from Cohen and Kurath [51]. The spectroscopic factor for ^{7}Li $\rightarrow$ ^{5}Li transfer is taken as 1.0. The finite range Distorted Wave Born Approximation (DWBA) formalism in the post form for stripping and prior form for pickup was used. Calculations were carried out including the full complex remnant term.

The optical model potential used in the entrance ^{7}Li+^{205}Tl channel [52] is found to explain the elastic scattering data at all the bombarding energies very well, shown as dashed line in Fig. 3. The CRC calculations for one neutron stripping, two neutron stripping and one neutron pickup are shown in Fig. 2(a-c). One neutron and two neutron stripping calculations are found to explain the data satisfactorily, while the one neutron pickup calculations underpredict the data. The underprediction of one neutron pickup might be due to lesser known spectroscopic information for ^{204}Tl [50].

3.2.2 CDCC calculations

To investigate the effect of projectile breakup on elastic scattering as well as for estimating the breakup cross sections, CDCC calculations have been carried out. The coupling scheme used in CDCC is similar to that described in our earlier works [21,55,56]. The calculations assumed a two-body $\alpha - t$ cluster structure for the ^{7}Li nucleus. The ground state and inelastic excitation of ^{7}Li (0.478 MeV, $\frac{1^-}{2}$) were considered as pure L = 1 cluster states, where L is the relative angular momentum of clusters. The continuum above the ^{7}Li$\rightarrow$ $\alpha + t$ breakup threshold (2.47 MeV) was discretized into bins of constant momentum width $k = 0.20$ fm^{-1}, where $\hbar k$ is the momentum of $\alpha + t$ relative motion. The binding potentials for all the bound and continuum cluster states were the well-known potentials from Ref. [57]. The cluster wave functions for each bin in the continuum were averaged over the bin width and each of these bins were then treated as an excited state of ^{7}Li with excitation energy equal to the mean of the bin energy range. The continuum momentum bins were truncated at the upper limits of $k_{max} = 0.8$ fm^{-1} for the calculations. The continuum states with relative orbital angular momentum L = 0, 1, 2, and 3 were included along with the $\frac{5^-}{2}$ and $\frac{7^-}{2}$ resonance states. In addition, the full continuum continuum couplings were taken into account in the final calculations. The real part of required fragment-target potentials $V_{\alpha-T}$ and V_{t-T} in cluster folding model were taken from S$\tilde{a}$o Paulo potential [58], while short range imaginary potential with values W_0 = 40 MeV, r_w = 1.00 fm, a_w = 0.40 fm was used.

The bare calculations (without including any continuum couplings) and the calculations with continuum couplings are shown as a dotted and solid lines respectively in Fig. 3. As can be seen, the coupling effects are evident at above barrier energies. The non-capture breakup (NCBU) cross sections were also obtained from these calculations.

Table 2 Potential parameters used in CRC calculations for ^{7}Li+^{205}Tl system. The radius parameters in the potentials are derived from $R_i = r_i A^{1/3}$, where i = R (Real), V (Volume), S (Surface), C (Coulomb) and A is the target mass number

System	V_R (MeV)	r_R (fm)	a_R (fm)	W_V (MeV)	r_v (fm)	a_v (fm)	W_s (MeV)	r_s (fm)	a_s (fm)	r_C (fm)	References
^{7}Li+^{205}Tl	179.64	1.24	0.85	23.41	1.59	0.59	35.51	1.18	0.87	1.802	[52]
^{6}Li+^{206}Tl	258.42	1.12	0.81	0.10	1.54	0.73	24.49	1.31	0.94	1.67	[53]
^{8}Li+^{204}Tl	167.10	1.23	0.79	27.45	1.80	0.53	28.14	1.46	0.92	1.57	[54]

Table 3 Energy levels of residual nuclei, spin-parity values and corresponding spectroscopic factors [46–50] used in the CRC calculations

^{206}Tl			^{207}Tl			^{204}Tl		
E	J^π	C^2S	E	J^π	C^2S	E	J^π	C^2S
(MeV)			(MeV)			(MeV)		
0.00	0^-	1	0.00	0.5^+	1.70	0.00	2^-	1.46
0.26	2^-	1	0.35	1.5^+	3.58	0.14	2^-	0.36
0.31	1^-	1	1.35	5.5^-	10.55	0.32	2^-	1.39
0.64	2^-	1	1.68	2.5^+	3.75	0.35	4^-	3.09
0.80	1^-	1				0.47	2^-	0.65
2.58	5^+	1				0.49	2^-	0.32
						0.54	2^-	0.038
						0.68	2^-	0.10
						0.76	2^-	0.15
						0.87	4^-	0.18
						0.97	4^-	0.23
						1.10	7^+	4.61
						1.25	2^-	0.12
						1.29	6^+	4.36
						1.40	2^-	0.02
						1.58	4^-	1.03
						1.70	5^-	1.54
						1.83	4^-	1.32
						1.93	4^-	0.35
						2.11	4^-	0.15
						2.23	4^-	0.76
						2.37	4^-	0.31
						2.48	4^-	0.20
						2.57	4^-	0.19
						2.67	4^-	0.14
						2.73	4^-	0.54
						2.83	2^-	0.02
						3.05	4^-	0.06

Table 4 The ground state Q values for neutron transfer reactions in the ^{7}Li+^{205}Tl system

Reaction	Residue	Q value (MeV)
(a) 1n Stripping	^{206}Tl	−0.7473
(b) 2n Stripping	^{206}Tl	0.4413
(c) 1n Pickup	^{204}Tl	−5.5134

3.3 Systematics of transfer cross sections with ^{7}Li projectile

The systematic of available neutron transfer (1n stripping, 2n stripping and 1n pickup) cross section data with ^{7}Li projectile on several (^{65}Cu [59], ^{93}Nb [60], ^{124}Sn [12], ^{197}Au [61], ^{198}Pt [62] and ^{209}Bi [63]) targets was presented in our previous work [21]. We have added the present cross section

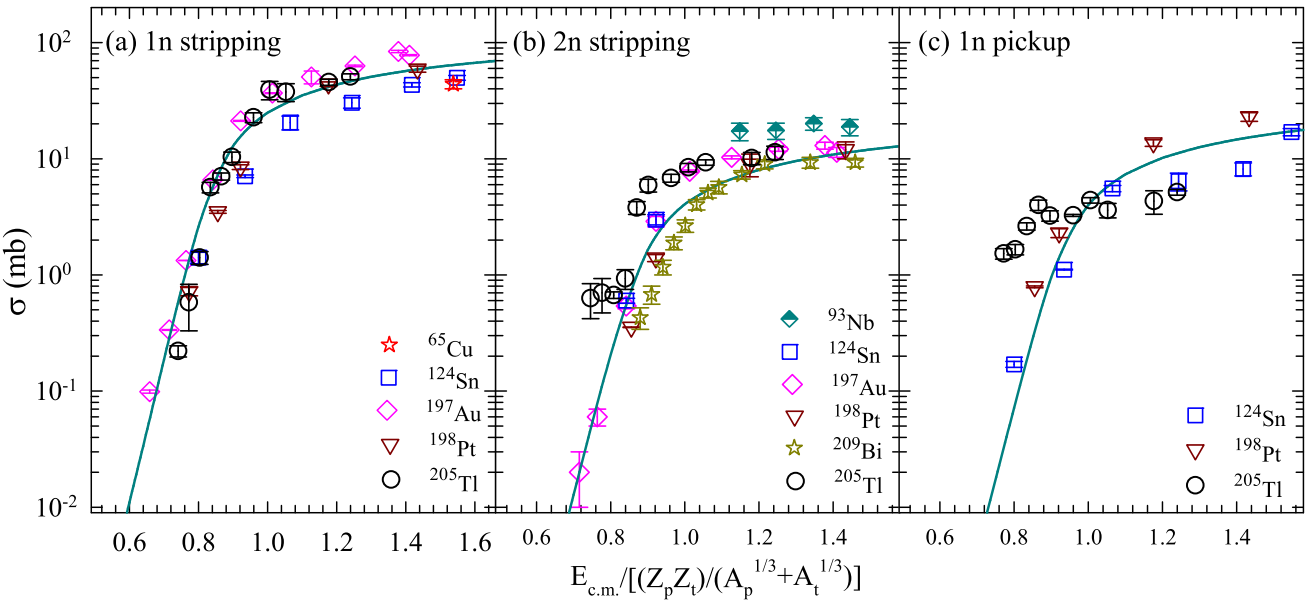

Fig. 4 Systematic behaviour of (**a**) one neutron stripping, (**b**) two neutron stripping and (**c**) one neutron pickup cross sections as a function of reduced energy with ^{7}Li projectile on various targets (adopted from Ref. [21]). Lines are same as in Ref. [21]

data for 1n stripping, 2n stripping and 1n pickup with ^{205}Tl target and shown in Fig. 4(a-c) respectively. As can be seen from the figure, the present data also agree with the universal behaviour in the cross sections in all the three plots. However, the trend of the 1n pickup cross sections is not reproduced by the universal function, particularly at low reduced energies. Similar systematic for neutron transfer cross sections was observed with ^{6}Li [22] and ^{9}Be [15,17] projectiles. In addition, a similar universal behaviour with weakly bound projectiles was also shown earlier for the inclusive α [6,60,64–66], fusion [6] and reaction cross sections [5].

3.4 Comparison of CF, ICF and neutron transfer cross sections with ^{7}Li projectile

It is interesting to compare the measured cumulative neutron transfer excitation function with the CF and ICF cross sections for the present system along with other targets where similar data is available for ^{7}Li induced reactions. Figure 5 (a-d) shows the comparison of neutron transfer, CF and ICF cross sections as a function of bombarding ^{7}Li energy for four (^{205}Tl, ^{198}Pt, ^{197}Au and ^{124}Sn) targets. A similar trend is observed in all the plots. The CF cross-sections are larger than ICF and neutron transfer at above barrier energies, while ICF dominates at below barrier energies followed by transfer cross section over the CF contribution. As the neutron separation energy ($S_n = 7.25$ MeV) is higher than the α separation energy ($S_\alpha = 2.45$ MeV) of ^{7}Li projectile, the ICF cross sections are higher than that of neutron transfer, indicating the dominant role of projectile structure in the reaction mechanism.

3.5 Reaction mechanism in the ^{7}Li+^{205}Tl system

For complete understanding the reaction mechanism in the ^{7}Li+^{205}Tl system, the measured CF, ICF and transfer cross sections and their sum are compared with the deduced reaction cross sections from the present calculations (using global optical model potential of Ref. [52]), shown in Fig. 6. The reaction cross sections obtained from the global optical model potential of Ref. [52] and from CDCC are found to be similiar (within 10%). A reasonable good agreement of reaction cross sections with the sum was observed at all the energies. In Fig. 6, the fusion cross sections calculated by the barrier penetration model (BPM) using bare potential in CDCC are also shown which reproduce the experimental Total Fusion (TF) at above barrier energies but underpredict at sub barrier energies. The cumulative absorption cross sections from CDCC calculations are found to agree with the TF transfer cross sections at higher energies. NCBU cross sections from CDCC calculations are also shown, which has lower contributions compared with CF, ICF and transfer cross sections.

4 Summary

In summary, we have measured one neutron stripping, two neutron stripping, and one neutron pickup cross sections near Coulomb barrier energies for ^{7}Li+^{205}Tl system using online γ-ray measurement technique. The measurements are compared with the CRC calculations by using the global optical model potential parameters. One neutron and two neutron

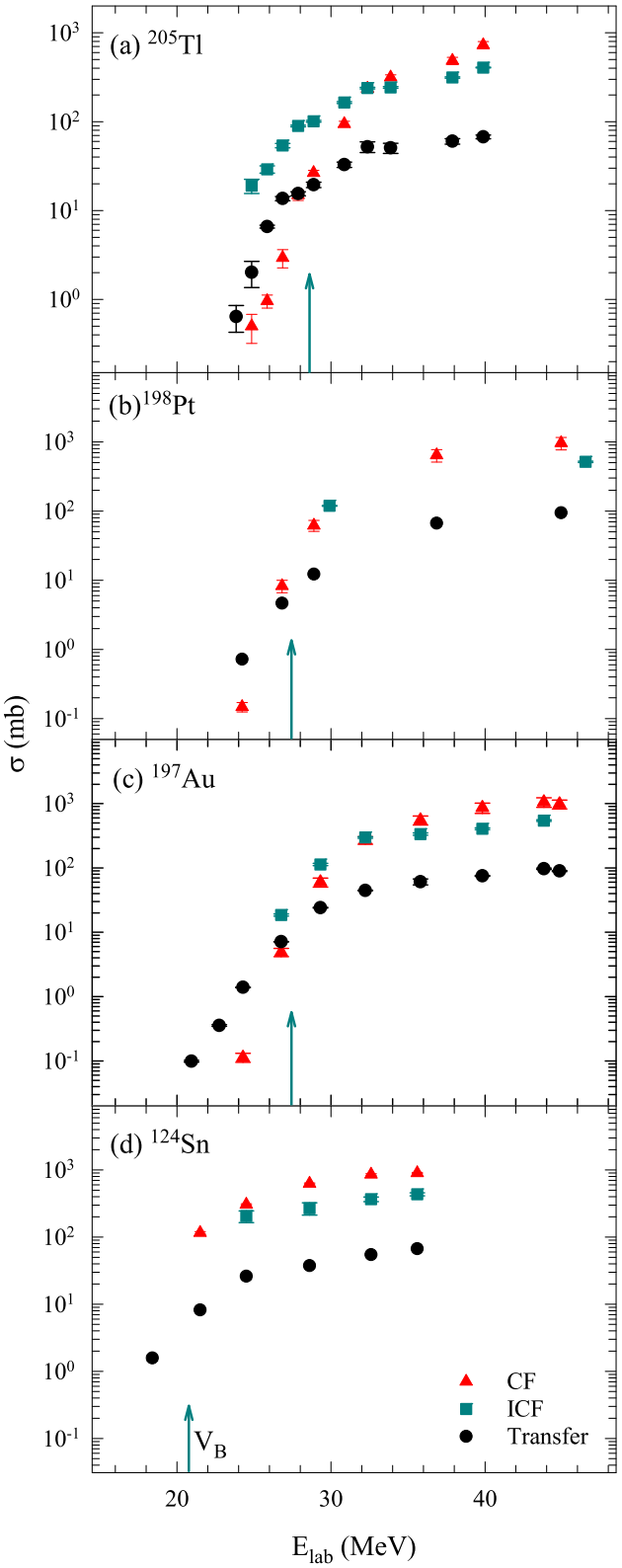

Fig. 5 The comparison of measured cumulative neutron transfer cross sections with CF and ICF cross sections for ^{7}Li induced reactions on (**a**)^{205}Tl [41], (**b**)^{198}Pt [9], (**c**)^{197}Au [10] and ^{124}Sn [12] targets. Dashed vertical line indicates Coulomb barrier energies of the respective systems

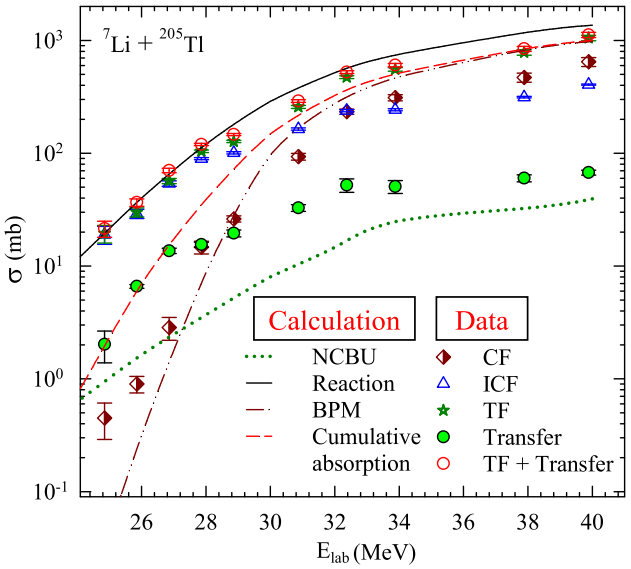

Fig. 6 Measured CF, ICF, transfer cross sections and their cumulative is compared with the reaction cross sections for the ^{7}Li+^{205}Tl system. NCBU, cumulative absorption, and BPM model calculations are also shown (see text for details)

stripping calculations are found to explain the data satisfactorily, while the one neutron pickup calculations underpredict the data. The elastic scattering data was also measured at three angles and was utilized for testing entrance channel potentials in the coupled channel calculations and also to get the reaction cross sections. The CDCC calculations were also performed assuming α+t cluster structure of ^{7}Li projectile and the effect of breakup on elastic scattering angular distribution as well as NCBU cross sections were estimated. The systematic of neutron transfer cross sections show an approximate universal behaviour. Comparison of the measured cumulative neutron transfer excitation function with the CF and ICF cross sections for the present system along with the literature data with ^{7}Li projectile shows dominance of CF cross sections at above barrier energies and ICF dominates at below barrier energies. Further, a cumulative of measured CF, ICF and neutron transfer cross sections shows reasonable good agreement with estimated reaction cross sections.

Acknowledgements The authors would like to thank the Pelletron-LINAC accelerator staff for the smooth operation of the accelerator during the experiment. We also thank Mr. P. Patale for help during the experiment. P.M. acknowledges the financial support of Board of Research in Nuclear Science (BRNS), India (Sanction No: 58/14/04/2019-BRNS/10254) and CSIR-UGC, India in carrying out these investigations. P.M. thank BARC for providing the facility to carry out the research work.

Funding Open access funding provided by Department of Atomic Energy.

Data Availability Statement Data will be made available on reasonable request [Author's comment: The datasets generated during and/or analysed during the current study are available from the corresponding author on reasonable request.].

Code Availability Statement My manuscript has no associated code/software. [Author's comment: Code/Software sharing not applicable to this article as no code/software was generated or analysed during the current study].

References

1. L.F. Canto, P.R.S. Gomes, R. Donangelo, M.S. Hussein, Phys. Rep. **424**, 1 (2006)
2. N. Keeley, R. Raabe, N. Alamanos, J.L. Sida, Prog. Part. Nucl. Phys. **59**, 579 (2007)
3. N. Keeley, N. Alamanos, K.W. Kemper, K. Rusek, Prog. Part. Nucl. Phys. **63**, 396 (2009)
4. L.F. Canto, P.R.S. Gomes, R. Donangelo, J. Lubian, M.S. Hussein, Phys. Rep. **596**, 1 (2015)
5. J.J. Kolata, V. Guimarães, E.F. Aguilera, Eur. Phys. J. A **52**, 123 (2016)
6. V. Jha, V.V. Parkar, S. Kailas, Phys. Rep. **845**, 1 (2020)
7. L.F. Canto, V. Guimarães, J. Lubián, M.S. Hussein, Eur. Phys. J. A **56**, 281 (2020)
8. M. K. Pradhan, A. Mukherjee, P. Basu, A. Goswami, R. Kshetri, Subinit Roy, P. Roy Chowdhury, M. Saha Sarkar, R. Palit, V. V. Parkar, et al., Phys. Rev. C **83**, 064606 (2011)
9. A. Shrivastava, A. Navin, A. Diaz-Torres, V. Nanal, K. Ramachandran, M. Rejmund, S. Bhattacharyya, A. Chatterjee, S. Kailas, A. Lemasson et al., Phys. Lett. B **718**, 931 (2013)
10. C.S. Palshetkar, S. Thakur, V. Nanal, A. Shrivastava, N. Dokania, V. Singh, V.V. Parkar, P.C. Rout, R. Palit, R.G. Pillay et al., Phys. Rev. C **89**, 024607 (2014)
11. S.P. Hu, G.L. Zhang, J.C. Yang, H.Q. Zhang, P.R.S. Gomes, J. Lubian, J.L. Ferreira, X.G. Wu, J. Zhong, C.Y. He et al., Phys. Rev. C **93**, 014621 (2016)
12. V. V. Parkar, Sushil K. Sharma, R. Palit, S. Upadhyaya, A. Shrivastava, S. K. Pandit, K. Mahata, V. Jha, S. Santra, K. Ramachandran, et al., Phys. Rev. C **97**, 014607 (2018)
13. V. V. Parkar, S. K. Pandit, A. Shrivastava, R. Palit, K. Mahata, V. Jha, K. Ramachandran, Shilpi Gupta, S. Santra, Sushil K. Sharma, et al., Phys. Rev. C **98**, 014601 (2018)
14. D.R. Otomar, J. Lubian, P.R.S. Gomes, T. Correa, J. Phys. G **40**, 125105 (2013)
15. Malika Kaushik, S. K. Pandit, V. V. Parkar, G. Gupta, S. Thakur, V. Nanal, H. Krishnamoorthy, A. Shrivastava, C. S. Palshetkar, K. Mahata, et al., Phys. Rev. C **104**, 024615 (2021)
16. Malika Kaushik, G. Gupta, V. V. Parkar, S. K. Pandit, Swati Thakur, V. Nanal, A. Shrivastava, R. G. Pillay, H. Krishnamoorthy, K. Mahata, et al., Eur. Phys. J. A **57**, 320 (2021)
17. Y. D. Fang, P. R. S. Gomes, J. Lubian, J. L. Ferreira, D. R. Mendes Junior, X. H. Zhou, M. L. Liu, N. T. Zhang, Y. H. Zhang, G. S. Li, et al., Phys. Rev. C **93**, 034615 (2016)
18. Prasanna M., V.V. Parkar, V. Jha, A. Parmar, B.A. Kanagalekar, B. Hegde, Nucl. Phys. A **1029**, 122570 (2023)
19. M. Fisichella, A.C. Shotter, P. Figuera, J. Lubian, A. Di Pietro, J.P. Fernandez-Garcia, J.L. Ferreira, M. Lattuada, P. Lotti, A. Musumarra et al., Phys. Rev. C **95**, 034617 (2017)
20. F. Gollan, D. Abriola, A. Arazi, M.A. Cardona, E. de Barbará, J. de Jesús, D. Hojman, R.M.I. Betan, J. Lubian, A.J. Pacheco et al., Phys. Rev. C **104**, 024609 (2021)
21. V. V. Parkar, A. Parmar, Prasanna M., V. Jha, and S. Kailas, Phys. Rev. C **104**, 054603 (2021)
22. V. V. Parkar, A. Parmar, P. M., V. Jha, and S. Kailas, Phys. Rev. C **107**, 024602 (2023)
23. P.H. Stelson, Phys. Lett. B **205**, 190 (1988)
24. P.H. Stelson, H.J. Kim, M. Beckerman, D. Shapira, R.L. Robinson, Phys. Rev. C **41**, 1584 (1990)
25. D. Shapira, P.H. Stelson, Phys. Rev. C **47**, 1666 (1993)
26. S. Kailas, A. Navin, Pramana **41**, 163 (1993)
27. A.M. Vinodkumar, A.K. Sinha, N.V.S.V. Prasad, K.M. Varier, P. Sugathan, Phys. Rev. C **54**, 791 (1996)
28. S. Appannababu, V.V. Parkar, V. Jha, S. Kailas, Phys. Rev. C **106**, 054612 (2022)
29. S. Appannababu, V.V. Parkar, V. Jha, S. Kailas, Eur. Phys. J. A **60**, 145 (2024)
30. G. Villanueva, A. Moro, J. Casal, J. Lei, Phys. Lett. B **855**, 138766 (2024)
31. Jin Lei and A. M. Moro, Phys. Rev. C **92**, 044616 (2015)
32. J. Lei, A.M. Moro, Phys. Rev. C **95**, 044605 (2017)
33. J. Lei, A.M. Moro, Phys. Rev. Lett. **123**, 232501 (2019)
34. J. Lei, A.M. Moro, Phys. Rev. C **108**, 034612 (2023)
35. V. Jha, V.V. Parkar, S. Kailas, Phys. Rev. C **89**, 034605 (2014)
36. V.V. Parkar, V. Jha, S. Kailas, Phys. Rev. C **94**, 024609 (2016)
37. V.V. Parkar, V. Jha, S. Kailas, EPJ Web Conf. **163**, 00044 (2017)
38. A.G. Camacho, J. Lubian, H.Q. Zhang, S.-G. Zhou, Chin. Phys. C **41**, 124103 (2017)
39. J. Lubian, J.L. Ferreira, J. Rangel, M.R. Cortes, L.F. Canto, Phys. Rev. C **105**, 054601 (2022)
40. J. Rangel, M. Cortes, J. Lubian, L. Canto, Phys. Lett. B **803**, 135337 (2020)
41. V. V. Parkar, Prasanna M., Ruchi Rathod, V. Jha, S. K. Pandit, A. Shrivastava, K. Mahata, K. Ramachandran, R. Palit, M. S. R. Laskar, et al., Phys. Rev. C **109**, 014610 (2024)
42. R. Palit, S. Saha, J. Sethi, T. Trivedi, S. Sharma, B. S. Naidu, S. Jadhav, R. Donthi, P. B. Chavan, H. Tan, et al., Nucl. Instrum. Meth. Phys. Res., Sect. A **680**, 90 (2012)
43. T.A. Berry, Z. Podolyák, R.J. Carroll, R. Lică, B.A. Brown, H. Grawe, C. Sotty, N.K. Timofeyuk, T. Alexander, A.N. Andreyev et al., Phys. Rev. C **101**, 054311 (2020)
44. R. Broda, K.H. Maier, B. Fornal, J. Wrzesiński, B. Szpak, M.P. Carpenter, R.V.F. Janssens, W. Królas, T. Pawłat, S. Zhu, Phys. Rev. C **84**, 014330 (2011)
45. I.J. Thompson, Comput. Phys. Rep. **7**, 167 (1988)
46. M.B. Lewis, W.W. Daehnick, Phys. Rev. C **1**, 1577 (1970)
47. P.D. Barnes, E.R. Flynn, G.J. Igo, D.D. Armstrong, Phys. Rev. C **1**, 228 (1970)
48. P. Grabmayr, A. Mondry, G.J. Wagner, P. Woldt, G.P.A. Berg, J. Lisantti, D.W. Miller, H. Nann, P.P. Singh, E.J. Stephenson, J. Phys. G : Nucl. Part. Phys. **18**, 1753 (1992)
49. H. Langevin-Joliot, E. Gerlic, J. Guillot, J. van de Wiele, J. Phys. G :Nucl. Part. Phys. **10**, 1435 (1984)

50. P. Smith, R. Peterson, R. Emigh, R. Anderson, Nucl. Phys. A **342**, 437 (1980)
51. S. Cohen, D. Kurath, Nucl. Phys. A **101**, 1 (1967)
52. Y. Xu, Y. Han, J. Hu, H. Liang, Z. Wu, H. Guo, C. Cai, Phys. Rev. C **97**, 014615 (2018)
53. Y. Xu, Y. Han, J. Hu, H. Liang, Z. Wu, H. Guo, C. Cai, Phys. Rev. C **98**, 024619 (2018)
54. X. Su, Y. Han, H. Liang, Z. Wu, H. Guo, C. Cai, Phys. Rev. C **95**, 054606 (2017)
55. V.V. Parkar, V. Jha, B.J. Roy, S. Santra, K. Ramachandran, A. Shrivastava, A. Chatterjee, S.R. Jain, A.K. Jain, S. Kailas, Phys. Rev. C **78**, 021601 (2008)
56. V. Jha, S. Kailas, Phys. Rev. C **80**, 034607 (2009)
57. B. Buck, A. Merchant, J. Phys. G:Nucl. Part. Phys. **14**, L211 (1988)
58. L. C. Chamon, B. V. Carlson, L. R. Gasques, D. Pereira, C. De Conti, M. A. G. Alvarez, M. S. Hussein, M. A. Cândido Ribeiro, E. S. Rossi, and C. P. Silva, Phys. Rev. C **66**, 014610 (2002)
59. A. Shrivastava, A. Navin, N. Keeley, K. Mahata, K. Ramachandran, V. Nanal, V.V. Parkar, A. Chatterjee, S. Kailas, Phys. Lett. B **633**, 463 (2006)
60. S.K. Pandit, A. Shrivastava, K. Mahata, V.V. Parkar, R. Palit, N. Keeley, P.C. Rout, A. Kumar, K. Ramachandran, S. Bhattacharyya et al., Phys. Rev. C **96**, 044616 (2017)
61. C. S. Palshetkar, Shital Thakur, V. Nanal, A. Shrivastava, N. Dokania, V. Singh, V. V. Parkar, P. C. Rout, R. Palit, R. G. Pillay, et al., Phys. Rev. C **89**, 024607 (2014b)
62. A. Shrivastava, A. Navin, A. Diaz-Torres, V. Nanal, K. Ramachandran, M. Rejmund, S. Bhattacharyya, A. Chatterjee, S. Kailas, A. Lemasson et al., Phys. Lett. B **718**, 931 (2013)
63. M. Dasgupta, P.R.S. Gomes, D.J. Hinde, S.B. Moraes, R.M. Anjos, A.C. Berriman, R.D. Butt, N. Carlin, J. Lubian, C.R. Morton et al., Phys. Rev. C **70**, 024606 (2004)
64. S. Santra, S. Kailas, V.V. Parkar, K. Ramachandran, V. Jha, A. Chatterjee, P.K. Rath, A. Parihari, Phys. Rev. C **85**, 014612 (2012)
65. V.V. Parkar, V. Jha, S. Kailas, Eur. Phys. J. A (Lett.) **59**, 88 (2023)
66. Satbir Kaur, V. V. Parkar, S. K. Pandit, A. Shrivastava, K. Mahata, K. Ramachandran, Sangeeta Dhuri, P. C. Rout, A. Kumar, and Shilpi Gupta, Nucl. Phys. A **1046**, 122864 (2024)